POROUS SILICON CARBIDE: A NEW THERMAL INSULATION MATERIAL FOR HARSH ENVIRONMENT MEMS

P.J. Newby[1,2,3], M. Aslaki[1,2], V. Aimez[1,2], and L.G. Fréchette[1,2]*

[1]Institut Interdisciplinaire d'Innovation Technologique (3IT), Université de Sherbrooke, 3000 Boulevard Université, Sherbrooke, J1K OA5, Québec, Canada

[2]Laboratoire Nanotechnologies Nanosystèmes (LN2)- CNRS UMI-3463, Université de Sherbrooke, 3000 Boulevard Université, Sherbrooke, J1K OA5, Québec, Canada

[3]Institut des Nanotechnologies de Lyon, Université de Lyon, CNRS, INSA de Lyon, Villeurbanne, France

ABSTRACT

In this work we demonstrate that porous SiC can be used as a thermal insulation material in MEMS. We have optimised the fabrication process of porous silicon carbide (PSiC), in order to fabricate thick uniform layers. The thermal conductivity of PSiC was measured using the "3 omega" method, showing that it is two orders of magnitude lower than that of bulk SiC. We also carried out chemical etching tests which demonstrate that PSiC has excellent chemical resistance to common cleanroom solvents and etchants. We also studied its high temperature behaviour, in O_2 and N_2, and our results indicate that PSiC is stable up to at least 1000°C. These two properties mean PSiC is compatible with most microfabrication processes, suggesting its applicability as a thermal insulation material, especially for harsh environment MEMS.

INTRODUCTION

Thermal insulation is essential in several types of MEMS (bolometers, PCR devices, or gas sensors for example). Depending on the device, effective thermal insulation can improve sensitivity, reduce power consumption, or decrease response time. Silicon is the substrate material of choice for most MEMS, but due to its high thermal conductivity (156 $W.m^{-1}.K^{-1}$ [1]), other materials or structures must be integrated to provide thermal insulation.

The most common solution is to place the element requiring insulation on a suspended membrane, but such structures are fragile, and impose limits on the design of the device [2]. An interesting approach, well known with silicon, is to locally reduce the thermal conductivity of the single-crystal substrate by selectively nanostructuring it into porous silicon through electrochemical etching [3]. The nanostructures which form porous Si have a characteristic size of approximately 10 nm, which is smaller than the mean free path of phonons in silicon. This causes phonon scattering, and due to this, the thermal conductivity of porous Si is 2-3 orders of magnitude lower than bulk Si [4]. However, porous Si is highly susceptible to chemical etching by many common microfabrication chemicals [5] (photoresist developer for example [6]) and cannot be used above 400°C, as its structure undergoes considerable reorganisation [7]. This is a major obstacle to its integration in a MEMS process flow. To avoid these problems, we propose to nanostructure a semiconductor with vastly superior physical properties: silicon carbide. Several groups have demonstrated that SiC can be nanostructured by making it porous [8]–[12], so in principle, the thermal conductivity of porous SiC (PSiC) should be significantly lower than that of bulk SiC, if the nanostructures are small enough. In order to be used for thermal insulation, porous SiC must not only have a low thermal conductivity, but must also be able to withstand standard microfabrication processes. This implies good chemical resistance and high temperature stability.

Although the fabrication of porous SiC has been demonstrated, these PSiC layers are generally non-uniform and not thick enough for thermal insulation applications. Furthermore, the current literature does not provide enough detail on the effect of fabrication parameters on the morphology of PSiC. The thermal conductivity of PSiC has never been measured to our knowledge, nor has its chemical resistance been characterised. A couple of groups have studied the high temperature behaviour of PSiC, but their results differ, and seem to be morphology dependent [13], [14]. As a consequence, this property must be characterised for our own samples.

We have carried out a systematic study of the fabrication process of PSiC. This study has led to a set of optimized parameters which enable the formation of thick uniform layers. We measured the thermal conductivity of PSiC, using the "3 omega" method, and showed that it is significantly lower than that of bulk SiC. We also carried out chemical etching tests which demonstrate that PSiC has excellent chemical resistance. Finally we studied its high temperature behaviour, in O_2 and N_2, and our results indicate that PSiC is stable up to at least 1000°C.

FABRICATION OF THICK UNIFORM POROUS SIC LAYERS

Porous SiC is made by electrochemical etching in a hydrofluoric acid (HF) based solution. This process is well known and has been described extensively in the case of porous *silicon* [15], [16], and is essentially the same for SiC. The electrolyte we used was a $(1:4:5)_{vol}$ solution of 48% HF, water, and absolute ethanol. The substrates used were n-type 4H or 6H wafers supplied by SiCrystal or Tankeblue. The current density can be varied to control porosity. The main difference with the fabrication of porous Si is that UV lamps can be used to create electron-hole pairs to facilitate etching. There is, however, some debate as to whether illumination is necessary [11], [12]. The last two parameters are variable, and details are specified below for each set of samples.

We carried out a systematic study of the effect of the fabrication parameters on the morphology of the porous SiC layers. These tests led to a set of parameters optimised for the fabrication of thick uniform PSiC layers. Figure 1 shows SEM pictures of a 108 µm thick and uniform layer. This sample was fabricated using a 6H substrate at a current density of 220 mA/cm^2. We also found that fabricating the samples in the dark, without UV illumination, favoured the uniformity of the PSiC layers. From the work on porous *silicon*, it is known that the use of rest times at zero-current during etching can improve the uniformity of the samples. This is also true for PSiC, and we found that the optimal parameter was a cycle of 1s etching followed by an 8s rest. These samples are thicker and more uniform than those published to date.

THERMAL CONDUCTIVITY MEASUREMENTS BY THE 3 OMEGA METHOD

The thermal conductivity of porous SiC was measured using the "3 omega" (3ω) method, initially developed by Cahill [17]. The method has since been used by many groups, and is well suited to thin films with low thermal conductivities [17]–[21]. To carry out the 3ω measurements, a metal line is deposited on the film to be

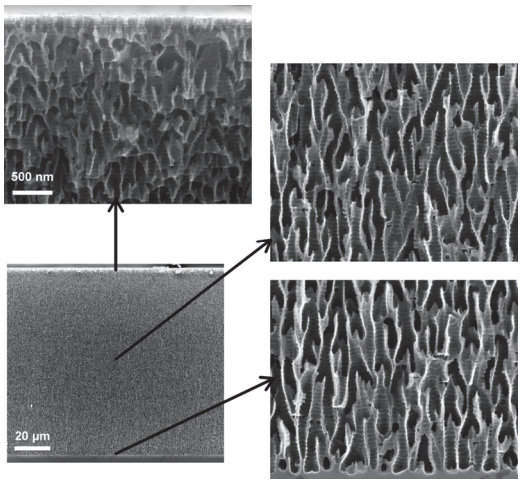

Figure 1: Porous SiC layer fabricated with optimised parameters. The layer is uniform and 108 µm thick. The scale is the same in all three zoomed-in images.

characterised. An alternating sine-wave current, of angular frequency ω, is applied to the line which, due to Joule heating, induces temperature oscillations, ΔT, at double the frequency (2ω). If the line is assumed to be infinitely long, the film thickness semi-infinite, and the frequency low, then the temperature oscillations can be approximated by:

$$\Delta T = \frac{P}{\pi k l}\left(-\frac{1}{2}\ln\omega - \frac{1}{2}\ln\frac{j2b^2}{D} + 0.922\right) \qquad (1)$$

where P is the electrical power, l the length of the line, k the thermal conductivity of the material on which the line is deposited, j the imaginary unit, $2b$ the line width, and D the thermal diffusivity of the material. This equation shows that ΔT varies linearly with ln ω, and its slope is inversely proportional to the thermal conductivity. The metal line has a resistance which varies with its temperature, and at the same frequency as ΔT (2ω). By applying Ohm's law to the metal line, we can show that the voltage of the line contains a third harmonic $V_{3\omega}$:

$$\Delta T = \frac{2V_{3\omega}}{\alpha V_0} \qquad (2)$$

where α is the temperature coefficient of resistance (TCR) of the metal line, and V_0 is the line's potential at the fundamental frequency ω. By combining eqs (1) and (2), the thermal conductivity of the material can be expressed as a function of experimentally measurable quantities:

$$k = -\frac{dR}{dT}\frac{V_{0\,RMS}I_{0\,RMS}^2}{4\pi l}\frac{\ln f_2 - \ln f_1}{V_{3w\,RMS_2} - V_{3w\,RMS_1}} \qquad (3)$$

where R is the resistance of the metal line, V_0 and I_0 the voltage and current amplitudes, and f its frequency.

In practice, $V_{3\omega}$ is measured as a function of the frequency of the sine current applied to the line, using a lock-in amplifier. When the frequency is low enough, $V_{3\omega}$ varies linearly with the logarithm of the frequency. The thermal conductivity of the material can be calculated from the slope of this linear section using equation (3).

The metal line is fabricated on the porous SiC layer by first depositing a thin SiO_2 layer by sputtering to prevent photoresist entering the pores in the subsequent photolithography [6]. The metal line is then made by evaporating 10 nm of chrome and 200 nm of gold and patterning it by lift-off photolithography. The line was 2.9 mm long, and either 4 or 20 µm wide, depending on the sample. The samples used in this case were thick layers (>100 µm), fabricated with the optimised parameters presented in the previous section.

Figure 2 shows an example of a curve obtained during the 3ω measurements. The depth at which thermal conductivity is measured by the 3ω method actually depends on the frequency of the sine current applied to the metal line. At lower frequencies, it is the bulk SiC substrate which is being measured, and at a higher frequency, the depth is shallower, and the thermal conductivity of the porous SiC is measured. This explains why there are two linear zones visible on the graph.

Based on our measurements, averaged over four different samples, we have measured a thermal conductivity of 5.8 $W.m^{-1}.K^{-1}$ ± 2.3 $W.m^{-1}.K^{-1}$. The samples all had a morphology like the sample presented in Fig. 1, and the porous layers had a thickness of ~100 µm. This represents a reduction of almost 2 orders of magnitude compared to bulk SiC. The presence of pores alone cannot account for such a strong reduction. As mentioned earlier, an additional reduction of thermal conductivity is caused by tortuosity and phonon scattering effects [4]. Indeed, the phonon mean free path in bulk SiC is 400 nm [22], and the size of the porous SiC nanostructures of our samples is on the order of 10 nm. Porosification of SiC has therefore been demonstrated to effectively reduce its thermal conductivity.

HIGH TEMPERATURE STABILITY

The aim of this test was to find the maximum temperature at which porous SiC could be used without modifications to its structure. The high temperature behaviour of PSiC was studied by annealing samples of different porosities at different temperatures and under O_2 and N_2.

Samples were made with three different porosity levels. The low, medium, and high porosity samples were made using the Si-face of, respectively 4H, 6H, and 4H substrates at current densities of respectively, 57, 220, and 360 mA/cm^2. All samples were made using UV illumination, and had a thickness of 10-20 µm. Annealing temperatures of 1000, 1200, and 1400°C were used. The furnace was heated at a speed of 20°C/minute, and once the target

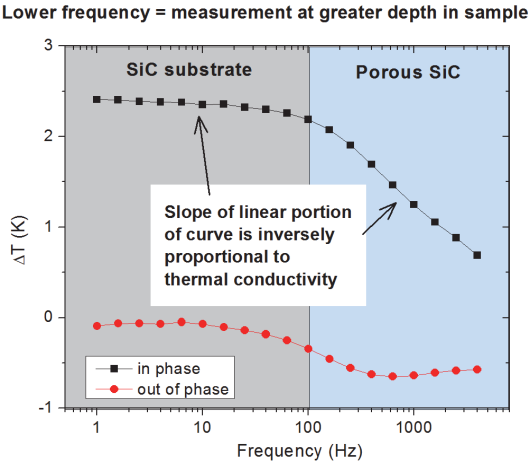

Figure 2: Example of a curve obtained during the 3ω measurements on PSiC.

temperature was reached, it was held for two hours. The samples were characterised by SEM imaging before and after annealing, in order to observe any structural modifications.

Figure 3 shows the results of N_2 annealing, for three porosity levels and different temperatures. Under N_2, the lowest porosity sample shows no sign of structural change, even after annealing at the highest temperature, 1400°C. At medium porosity, the porous structure is unchanged after annealing at 1200°C, but has changed significantly after annealing at 1400°C. This reorganisation was accompanied by a slight reduction of the thickness of the PSiC layer, of ~1 µm, for an initial thickness of 10 µm. The structure of the high porosity sample shows slight signs of reorganisation after the 1200°C anneal.

Figure 4 shows the results of O_2 annealing. After annealing, the nanostructures of the low porosity sample have swelled. At medium porosity, there is no visible change after annealing at 1000°C, but significant swelling has occurred after annealing at 1200°C. The thickness of the low and medium porosity layers did not vary following annealing at 1000 or 1200°C. The structure of the high porosity samples has swelled slightly after annealing at 1000°C. At 1200°C, the structure significantly reorganised and the thickness of the sample was half its initial value.

Swelling of the PSiC nanostructures after annealing under O_2 is inevitable, as SiC is oxidised by oxygen. However, only the structure of the high porosity sample was reorganised after annealing at 1200°C, as evidenced by the reduction of sample thickness, which was not observed for the other samples annealed in oxygen. For both oxygen and nitrogen annealing, our results show that the lowest porosity samples are stable up to higher temperatures, remaining stable up to 1400°C under N_2 and 1200°C under O_2. In all cases, the PSiC samples are stable up to at least 1000°C, suggesting compatibility with a broad range of thermal processes and high temperature SiC MEMS operation. There were probably changes in the surface chemistry of the samples at lower temperatures, but it was not the aim of this study to characterise these effects.

CHEMICAL RESISTANCE

Chemical resistance was tested in a selection of aggressive chemicals commonly used in microfabrication. These products are listed in Table 1 and cover the main operations where chemical solutions are used, *i.e.* cleaning, photolithography and wet etching. The samples were made from 4H substrates on the Si-face. To test

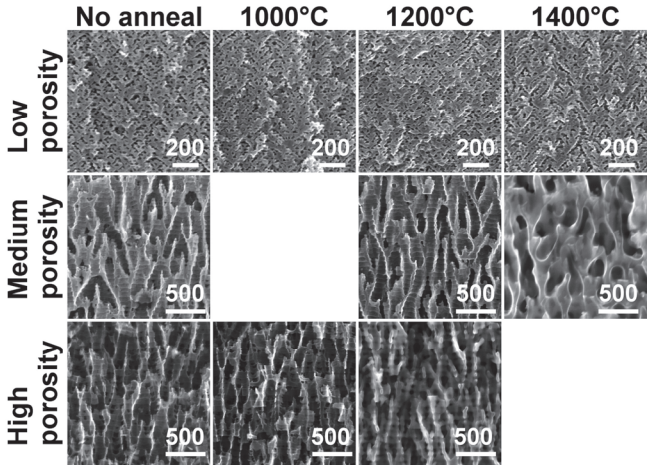

Figure 3: SEM cross-section images of porous SiC samples, before and after annealing under N_2.

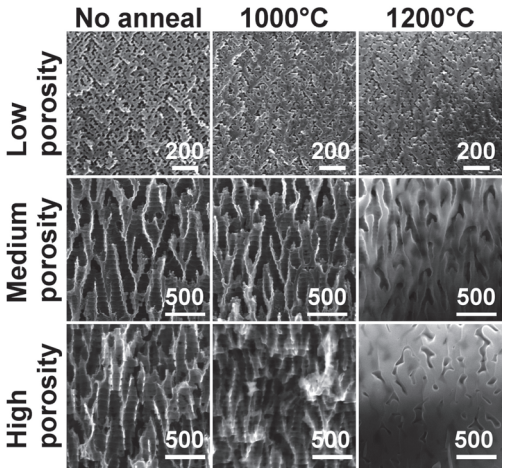

Figure 4: SEM cross-section images of porous SiC samples, before and after annealing under O_2.

the effect of porosity, the samples used were bi-layers formed of a high porosity layer (~19 µm thick) above a low porosity layer (~14 µm thick). The former was made at a current density of 360 mA/cm^2, and the latter at 47 mA/cm^2, and were fabricated under UV illumination. As long as the samples showed no signs of chemical etching, they were reused for other tests, but were dipped in HF first to remove any oxides grown on the surface. In order to detect any chemical etching, the samples were weighed before and after each etch, and SEM imaging was used before the first etch and after the last.

Table 1 shows the chemical solutions to which the porous SiC samples were exposed, the exposure time, and the measured mass variation. The mass variation is expressed in porosity points (for example, a change in porosity of 79% to 80% porosity corresponds to a 1 pp variation). None of the products tested showed any signs of chemical etching, except for RCA-SC1, which caused a slight variation of -2 pp after an exposure of 1h30. SEM imaging of the samples before and after exposure showed no visible signs of chemical etching, for all samples and products. No other signs of etching (*e.g.* bubbles, change of colour) were observed, for all the products tested. The variation of -2 pp observed for RCA-SC1 is only slightly above the measurement resolution. Furthermore, this occurred after an exposure of 1h30, whereas a typical RCA clean would last 10-15 min. Therefore, for all practical applications, porous SiC can be considered inert in RCA-SC1.

The exposure time was variable and was partly dictated by security considerations. In all cases, it was at least equal to a typical exposure time, and often greater. Given the thickness of the samples and the resolution of the balance used, the smallest measurable variation of porosity was 1.4 pp.

In conclusion, porous SiC is practically inert in all the products tested, which cover a wide variety of common microfabrication processes. Combined to its stability up to at least 1000°C, this means that PSiC is compatible with the majority of typical microfabrication processes, and can therefore be integrated into existing MEMS fabrication process flows without having to modify them. Furthermore, this means that porous SiC should be suitable for a variety of applications in harsh environments.

CONCLUSION

We have optimised the fabrication of porous SiC in order to fabricate uniform and very thick layers (up to 108 µm). For the first time, we have demonstrated that porous SiC is chemically inert in

Table 1: Mass variation of PSiC after exposure to common microfabrication chemicals, expressed in porosity points.

	Solution	Exposure time	Mass variation
Cleaning	Piranha	15 min	0
	HF 49%	1 h 13 min	0
	RCA-SC1 75°C	1 h 30 min	-2 pp
	RCA-SC2 75°C	1 h 05 min	0
Photolitho-graphy	MF-319	5 h 28 min	0
	AZ400K - H_2O $(1:4)_{vol}$	17 h 28 min	0
	SU-8 developer	24 h 33 min	0
Wet etching	KOH – H_20 $(1:4)_{vol}$ 70°C	24 h 09 min	0
	HF-HNO_3 $(9:4)_{vol}$ 52°C	1 h	0
	HF-HNO_3-CH_3COOH $(4.5:7.5:8)_{vol}$	1h 10 min	0
	Aqua regia	2 h 05 min	0

common microfabrication solutions, and measured its thermal conductivity. We have also demonstrated that its structure is stable up to at least 1000°C. Therefore porous SiC is a material which is highly suitable for thermal insulation in MEMS, as it is compatible with microfabrication processes, and is ready to be integrated into existing processes and devices, especially harsh environment MEMS.

ACKNOWLEDGEMENTS

The authors would like to thank the Rhône-Alpes region (France), NSERC, FQRNT, the Canada Research Chair program, and NanoQuébec for funding.

REFERENCES

[1] C. J. Glassbrenner and G. A. Slack, "Thermal conductivity of silicon and germanium from 3 K to the melting point," Physical Review, 134, A1058 (1964).

[2] R. M. Tiggelaar, P. van Male, J. W. Berenschot, J. G. E. Gardeniers, R. E. Oosterbroek, M. H. J. M. de Croon, J. C. Schouten, A. van den Berg, and M. C. Elwenspoek, "Fabrication of a high-temperature microreactor with integrated heater and sensor patterns on an ultrathin silicon membrane," Sensors and Actuators A: Physical, 119, 196 (2005).

[3] V. Lysenko, S. Perichon, B. Remaki, and D. Barbier, "Thermal isolation in microsystems with porous silicon," Sensors and Actuators A: Physical, 99, 13 (2002).

[4] G. Gesele, J. Linsmeier, V. Drach, J. Fricke, and R. Arens-Fischer, "Temperature-dependent thermal conductivity of porous silicon," Journal of Physics D: Applied Physics, 30, 2911 (1997).

[5] D. Hamm, T. Sakka, and Y. H. Ogata, "Etching of porous silicon in basic solution," Physica Status Solidi (a), 197, 175 (2003).

[6] M. Lai, G. Parish, Y. Liu, J. M. Dell, and A. J. Keating, "Development of an Alkaline-Compatible Porous-Silicon Photolithographic Process," Journal of Microelectromechanical Systems, 20, 418 (2011).

[7] R. Herino, A. Perio, K. Barla, and G. Bomchil, "Microstructure of porous silicon and its evolution with temperature," Materials Letters, 2, 519 (1984).

[8] J. S. Shor and A. D. Kurtz, "Photoelectrochemical Etching of 6H-SiC," Journal of the Electrochemical Society, 141, 778 (1994).

[9] M. Mynbaeva, "Porous SiC - Prospective Applications (Invited)," in MRS Proceedings, 742, K6.6 (2002).

[10] S. Zangooie, P. O. A. Persson, J. N. Hilfiker, L. Hultman, and H. Arwin, "Microstructural and infrared optical properties of electrochemically etched highly doped 4H-SiC," Journal of Applied Physics, 87, 8497 (2000).

[11] P. Newby, J.-M. Bluet, V. Aimez, L. G. Fréchette, and V. Lysenko, "Structural properties of porous 6H silicon carbide," Physica Status Solidi (c), 8, 1950 (2011).

[12] G. Gautier, J. Biscarrat, D. Valente, T. Defforge, A. Gary, and F. Cayrel, "Systematic Study of Anodic Etching of Highly Doped N-type 4H-SiC in Various HF Based Electrolytes," Journal of the Electrochemical Society, 160, D372 (2013).

[13] M. Mynbaeva, A. Lavrent'ev, I. Kotousova, A. Volkova, K. Mynbaev, and A. Lebedev, "On Current Limitations in Porous SiC Applications," Materials Science Forum, 483-485, 269 (2005).

[14] J. Bai, G. Dhanaraj, P. Gouma, M. Dudley, and M. Mynbaeva, "Porous SiC for HT Chemical Sensing Devices: an Assessment of its Thermal Stability," Materials Science Forum, 457-460, 1479 (2004).

[15] M. J. Sailor, "Porous Silicon in Practice." Weinheim: Wiley-VCH (2012).

[16] V. Lehmann, "Electrochemistry of silicon: instrumentation, science, materials and applications." Weinheim, Allemagne: Wiley-VCH (2002).

[17] D. G. Cahill, "Thermal conductivity measurement from 30 to 750 K: the 3ω method," Review of Scientific Instruments, 61, 802 (1990).

[18] N. O. Birge, "Specific-heat spectroscopy of glycerol and propylene glycol near the glass transition," Physical Review B, 34, 1631 (1986).

[19] N. O. Birge and S. R. Nagel, "Wide-frequency specific heat spectrometer," Review of Scientific Instruments, 58, 1464 (1987).

[20] D. G. Cahill, "Erratum: ``Thermal conductivity measurement from 30 to 750 K: The 3ω method'' [Rev. Sci. Instrum. 61, 802 (1990)]," Review of Scientific Instruments, 73, 3701 (2002).

[21] I. K. Moon, Y. H. Jeong, and S. I. Kwun, "The 3ω technique for measuring dynamic specific heat and thermal conductivity of a liquid or solid," Review of Scientific Instruments, 67, 29 (1996).

[22] E. Ziambaras and P. Hyldgaard, "Phonon Knudsen flow in nanostructured semiconductor systems," Journal of Applied Physics, 99, 054303 (2006).

CONTACT

*P.J. Newby, Pascal.Newby@USherbrooke.ca